



ELSEVIER

Physics Letters B 540 (2002) 199–206

PHYSICS LETTERS B

[www.elsevier.com/locate/npe](http://www.elsevier.com/locate/npe)

## Effect of E1 decay in the population of superdeformed structures

G. Benzoni<sup>a</sup>, A. Bracco<sup>a</sup>, F. Camera<sup>a</sup>, S. Leoni<sup>a</sup>, B. Million<sup>a</sup>, A. Maj<sup>b</sup>, A. Algora<sup>c</sup>,  
A. Axelsson<sup>d</sup>, M. Bergström<sup>e</sup>, N. Blasi<sup>a</sup>, M. Castoldi<sup>f</sup>, S. Frattini<sup>a</sup>, A. Gadea<sup>c</sup>,  
B. Herskind<sup>e</sup>, M. Kmiecik<sup>b</sup>, G. Lo Bianco<sup>g</sup>, J. Nyberg<sup>d</sup>, M. Pignanelli<sup>a</sup>, J. Styczen<sup>b</sup>,  
O. Wieland<sup>a</sup>, M. Zieblinski<sup>b</sup>, A. Zucchiatti<sup>f</sup>

<sup>a</sup> Dipartimento di Fisica, Università di Milano and INFN, via Celoria 16, 20133 Milano, Italy

<sup>b</sup> Niewodniczanski Institute of Nuclear Physics, 31-342 Krakow, Poland

<sup>c</sup> Laboratori Nazionali di Legnaro, via Romea, Legnaro (PD), Italy

<sup>d</sup> Department of Neutron Research, Uppsala University, S-75121 Uppsala, Sweden

<sup>e</sup> The Niels Bohr Institute, Blegdamsvej 15-17, 2100, Copenhagen, Denmark

<sup>f</sup> INFN sezione di Genova, Genova, Italy

<sup>g</sup> Dipartimento di Fisica, Università di Camerino e INFN Perugia, Camerino, Italy

Received 1 February 2002; received in revised form 13 June 2002; accepted 21 June 2002

Editor: V. Metag

### Abstract

Spectra of the yrast and excited superdeformed bands, forming the E2 quasi-continuum, are measured with the EUROBALL array for the nucleus  $^{143}\text{Eu}$ , in coincidence with high-energy  $\gamma$ -rays ( $E_\gamma > 3$  MeV). It is found that the intensity population of the superdeformed states is enhanced by a factor of  $\approx 1.6$  when a coincidence with a  $\gamma$ -ray with energy  $> 6$  MeV is required, in reasonable agreement with the increase of the line shape of the Giant Dipole Resonance built on a superdeformed configuration. This result shows that when an high energy E1  $\gamma$ -ray is involved in the decay it is more likely connected with a SD rather than a ND nucleus. In addition, the analysis of the rotational quasi-continuum suggests the presence of a superdeformed component. The data are also compared and found consistent with simulation calculations of the relative intensities of the SD states, including the E1 decay of superdeformed nature. © 2002 Elsevier Science B.V. All rights reserved.

PACS: 21.10.Tg; 21.10.Re; 21.60.Ka; 23.20.En; 23.20.L

The study of nuclear structure at the extreme limits of rotational stress and large shape changes has been a topic extensively investigated in the last years [1,2]. Gamma spectroscopy measurements have identified superdeformed (SD) rotational bands in more than 50 nuclei in several different mass regions

[3]. While the nature of SD bands has been interpreted in terms of the occupancy of a number of high- $N$  intruder orbitals ( $N$  being the major oscillator quantum number) only in a small number of cases [4–6] it has been possible to make firm assignments of spins, parities and excitation energies from observed single-step connections with normal deformed (ND) yrast states, as a consequence of the highly fragmented decay-out of the SD states.

E-mail address: [silvia.leoni@mi.infn.it](mailto:silvia.leoni@mi.infn.it) (S. Leoni).

Another relevant open question concerning the problem of superdeformation is the understanding of the population mechanisms of the SD states, having important consequences on the size of the intensities of the measured transitions of the SD bands. In fact, it has been found that the typical measured intensities of the SD bands are approximately 2 order of magnitude stronger than those measured at the same highest spins in normally deformed nuclei [7,8]. It has been suggested that such intense population of the SD band at high spins could be related to the E1 feeding of these states, which is expected to be strongly affected by the shape of the giant dipole resonance (GDR) strength function. As a consequence of the large nuclear prolate deformation, the GDR strength function is predicted to display a low energy component (corresponding to the dipole oscillation along the long symmetry axis) at an energy close to the neutron binding energy and exhausting one third of the total energy weighted sum rule strength [9]. This enhanced E1 strength together with the reduced level density of the SD states, as compared to the case of normal deformed nuclei, are expected to enhance the population of SD rotational bands. This mechanism has been originally proposed in Ref. [10] in connection with the understanding of the measured intensities of the SD yrast band of the nucleus  $^{152}\text{Dy}$ .

For a full understanding of the population mechanism of the SD configuration one would need to measure the absolute population probability for  $\gamma$  and particle feeding as a function of particle and  $\gamma$ -ray energy. In the present case we focus only on the E1 feeding by testing whether or not when an high energy E1  $\gamma$ -ray is involved in the decay it is more likely connected with a SD rather than a ND nucleus. In particular, the population of the SD structures is expected to increase with  $\gamma$ -ray energies, as a consequence of the GDR line shape built on a superdeformed nucleus. This is in general a difficult experimental task, due to both the exponential decrease of the yield of the high-energy  $\gamma$ -rays and to the weak intensity of the SD transitions, being at most of the order of few percent for the yrast band. However, due to the interest to this problem, already a decade ago, when the available detection arrays were at the limit to address this question, few experimental attempts were made in connection with superdeformed Gd isotopes [11–13], which did not show the behaviour predicted for the  $^{152}\text{Dy}$  case [10]. Presently, it is

not clear whether such discrepancy is due to a different mechanism than the originally proposed E1 decay (such as, for example, an enhanced neutron emission probability due to smaller level density in the superdeformed nucleus), or to the experimental conditions. The latter could be related to the choice of the bombarding energy and to the efficiency of the apparatus, which were not optimal to address the problem. Therefore, the population mechanism of the SD states still represents an interesting open problem in the study of superdeformation.

In this Letter the role of the E1 decay in the population of superdeformed structures is investigated with the more sensitive EUROBALL set up and in the case of another nucleus of similar mass,  $^{143}\text{Eu}$ . This nucleus has been chosen not only because it has a rather strong SD yrast line (of the order of 2% of the total nucleus population), but also rotationally correlated transitions forming a rather intense quasi-continuum structure of superdeformed character [14–16]. The aim of this work is to measure SD transitions (yrast and quasi-continuum) in coincidence with high-energy  $\gamma$ -rays and to study the dependence of their intensities as a function of the  $\gamma$ -ray energies in the interval 3–8 MeV. In this region one can probe the low energy tail of the GDR strength function that in a spherical nucleus is characterized by a Lorentzian shape centered at 14–15 MeV, while in the case of a superdeformed nucleus one third of the strength is expected to be around 10.5 MeV [9]. At variance from previous works on Gd isotopes, the bombarding energy of the projectile has been chosen to be 5 MeV larger than in the study of the SD yrast line [17], in order to have an entry distribution for the population of the  $^{143}\text{Eu}$  nucleus extending at higher temperature. This increases the phase space for the decay with high energy  $\gamma$ -rays. In addition, this work is also intended to provide a further verification of the superdeformed nature of the E2 quasi-continuum by determining whether or not the intensity of the spectral structures behave as a function of high-energy  $\gamma$ -rays similarly to the yrast line.

The experiment was performed at the Tandem Accelerator Laboratory of Legnaro (Padova). The  $^{37}\text{Cl}$  beam, at the incident energy of 165 MeV, impinged on a target of  $^{110}\text{Pd}$  (97.3% pure and  $950\ \mu\text{g}/\text{cm}^2$  thick) with a Au backing of  $15\ \text{mg}/\text{cm}^2$ . The chosen bombarding energy represents a good compromise for a good population of the SD band and for

E1 emission from the final residual nucleus at excitation energies around the binding energy. The compound nucleus  $^{147}\text{Eu}$  was formed at an excitation energy of 79 MeV. The maximum angular momentum is predicted to be  $68\hbar$  by the heavy-ion grazing model, in which the excitation of collective modes is taken into account in the fusion process [18]. This exceeds the angular momentum limit where fission becomes dominant. High-energy  $\gamma$ -rays were detected in the 8  $\text{BaF}_2$  scintillators of the HECTOR array [19] placed at 30 cm from the target center, shielded by lead to attenuate low-energy  $\gamma$ -rays. In addition, 4 small  $\text{BaF}_2$  detectors were placed with their front face at the outer surface of the target chamber to measure the time of flight with good resolution, information needed to reject neutron events. The time of flight of the Ge detectors was also measured relative to these small  $\text{BaF}_2$  detectors. The gain of each  $\text{BaF}_2$  detector has been monitored continuously during all the experiment using a LED source and small shifts were corrected during the off-line analysis. The calibration of the HPGe EUROBALL detectors was obtained using standard radioactive sources while the large volume  $\text{BaF}_2$  detectors were calibrated using the 15.1 MeV  $\gamma$  produced by the reaction  $^{11}\text{B} + D \rightarrow ^{12}\text{C}^* + n$ . We have accumulated events containing coincidences among a high-energy  $\gamma$ -ray ( $E_\gamma > 3$  MeV) measured in the  $\text{BaF}_2$  detectors and  $\gamma$ -rays detected in HPGe detectors, with the condition that at least 3 Ge detectors (without Compton suppression) had fired. The coincidence fold distribution for Ge detectors measured in the experiment has an average value at  $\approx 3$ , after Compton suppression.

The effect of the E1 population of the superdeformed yrast band by the  $\gamma$ -decay of the giant dipole resonance built on a superdeformed nucleus is investigated by measuring the relative intensity of the SD band at different values of the high-energy gating  $\gamma$ -rays. In Fig. 1 the spectrum of the superdeformed yrast transitions is shown for three different gating conditions on the high-energy  $\gamma$ -rays measured in the  $\text{BaF}_2$  scintillator detectors, namely  $3 < E_\gamma < 4$  MeV, corresponding to the average energy  $\langle E_\gamma \rangle = 3.4$  MeV (panel (a)),  $5 < E_\gamma < 6$  MeV, corresponding to  $\langle E_\gamma \rangle = 5.4$  MeV (panel (b)) and  $6 < E_\gamma < 14$  MeV, which due to the exponential nature of the spectrum corresponds to  $\langle E_\gamma \rangle = 7.3$  MeV (panel (c)). Each spectrum was obtained starting from a  $\gamma$ - $\gamma$  matrix

Doppler corrected on event-by-event basis according to the fractional Doppler shift of the superdeformed yrast band [21], and gated on the SD yrast and on the high-energy  $\gamma$ -rays. The single spectra are the sum of one-dimensional (1D) projections of such matrices (background subtracted with the Radware method [20]), obtained by gating in addition on the cleanest SD lines (namely 732, 794, 973, 1032, 1091, 1149, 1208, 1266, 1325, 1384, 1444, 1502, 1564, 1624, and 1684 keV). Since the SD gates used in the construction of the spectra have been placed all over the SD band, the extracted intensity of the SD yrast can only be used to study its relative behaviour and not to deduce an absolute value. To show the three spectra of Fig. 1 on the same scale, the data in panels (a) and (b) have been scaled down by a factor giving the same counts in the 917 keV low spin transition between spherical states, as collected with the high-energy gating condition  $\langle E_\gamma \rangle = 7.3$  MeV (panel (c)). In all three cases the SD yrast transitions of interest are marked by diamonds and can be identified even when the statistics is largely reduced as in the case of the gating condition  $6 < E_\gamma < 14$  MeV (panel (c)). Due to the exponential nature of the high energy  $\gamma$ -ray spectrum it was not possible to measure with significant statistics the SD yrast lines gated by  $\gamma$  transitions larger than 8 MeV. As one can see from the figure (with the help of the horizontal lines at 100 and 200 counts), the intensities of the SD peaks grow with increasing energy of the gating  $\gamma$ -rays. The increase of the SD yrast population as function of the high-energy transition was evaluated by summing the intensity (after subtraction of the background between the peaks and efficiency correction) of the SD lines marked in the figure. The deduced values were normalized to that corresponding to the 3.4 MeV high-energy gating condition and the error bars have been evaluated taking into account both the statistical error and the uncertainty related to different low lying ND transitions which can be used to normalize the spectra. The resulting increase between the lowest and the highest gating condition is approximately a factor of 1.6 (as it will be later discussed in connection with Fig. 4), in agreement with the enhancement obtained by using the well defined 973 keV SD yrast line only (shown by the cross in Fig. 4).

In the  $^{143}\text{Eu}$  nucleus unresolved transitions from discrete excited rotational bands form a well identi-

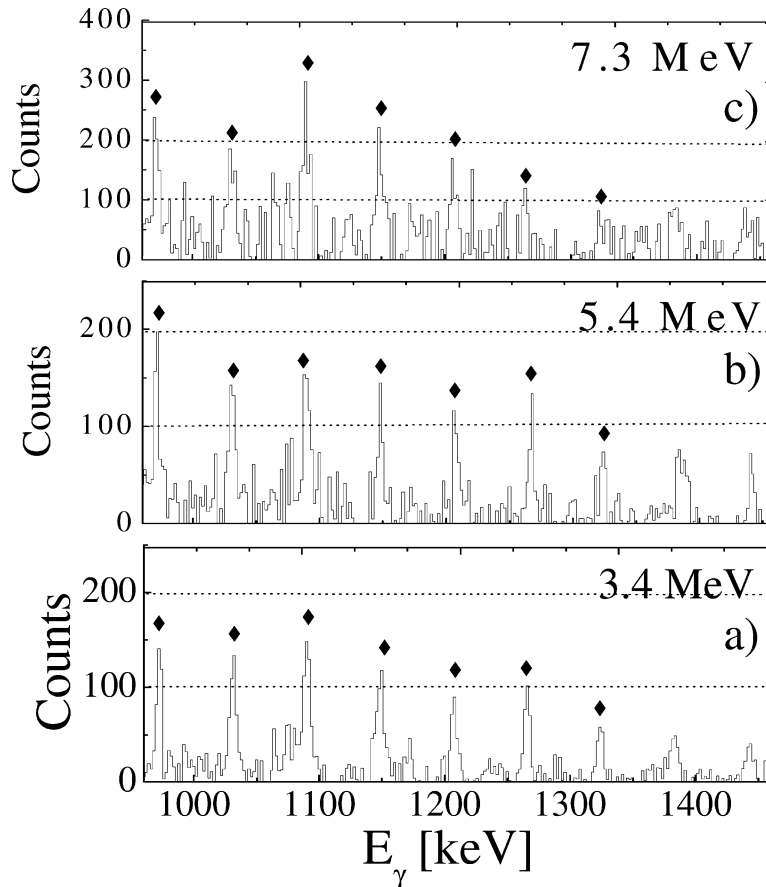


Fig. 1. Spectra of the SD yrast band of  $^{143}\text{Eu}$ , gated by high-energy  $\gamma$ -rays with average energies  $\langle E_\gamma \rangle = 3.4, 5.4$  and  $7.3$  MeV (panel (a), (b) and (c), respectively). The spectra are normalized to the intensity of the low spin 917 keV line with the gating condition  $\langle E_\gamma \rangle = 7.3$  MeV. The horizontal lines at 100 and 200 counts help the comparison of the SD lines intensities in the different spectra.

fied ridge structure in  $\gamma$ - $\gamma$  spectra. In Fig. 2 one-dimensional projections on a 60 keV wide strip perpendicular to the main diagonal of the  $E_{\gamma 1} \times E_{\gamma 2}$  matrix at the average transition energy  $(E_{\gamma 1} + E_{\gamma 2})/2 = 1140$  keV are shown, for average gating transitions of  $\langle E_\gamma \rangle = 3.4, 4.4$  and  $6.2$  MeV (panel (a), (b) and (c), respectively), corresponding to the energy intervals  $3 < E_\gamma < 4$  MeV,  $4 < E_\gamma < 5$  MeV and  $5 < E_\gamma < 14$  MeV. In this connection, it is important to notice that since the ridge structure can only be identified in  $\gamma$ - $\gamma$  matrices, the statistics is reduced as compared to the previous one-dimensional analysis of the SD yrast. Therefore, the analysis of the ridges could only be performed with the three high-energy gating conditions previously given. In the  $\gamma$ - $\gamma$  spectra the background has been reduced by subtracting a matrix of uncorre-

lated events constructed using the COR treatment of Ref. [22], with a COR reduction factor of 0.95, emphasizing the high spin region. The spectra are normalized to the intensity collected in the valley region of the spectrum gated by  $\langle E_\gamma \rangle = 6.2$  MeV. The superdeformed nature of the ridge structure is confirmed by the distance between the two most inner ridges ( $2 \times 4\hbar^2/\mathfrak{I}^{(2)} \approx 120$  keV, as indicated in the figure), which corresponds to a value of the dynamical moment of inertia very close to the one of the SD yrast line. In addition, the measurement of the lifetime of the ridge structure gives a quadrupole moment ranging from 10 to 13 eb, consistent with the deformation of the SD yrast [16]. The effect on the ridge structure produced by the requirement of detecting a transition with  $5 < E_\gamma < 14$  MeV can be seen by comparing

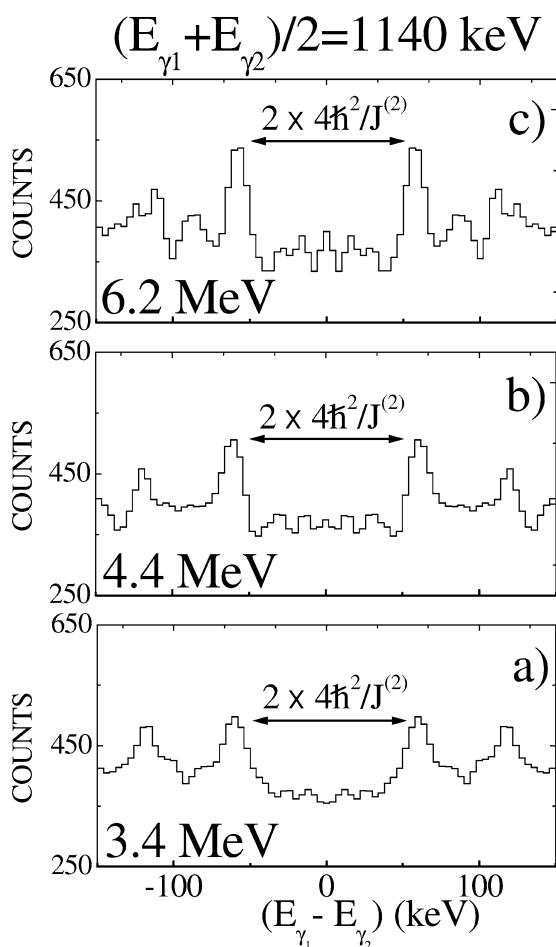


Fig. 2. Ridge structures observed at the average transition energy  $(E_{\gamma_1} + E_{\gamma_2})/2 = 1140$  keV in the  $\gamma$ - $\gamma$  matrix of  $^{143}\text{Eu}$  gated by high-energy transitions with  $\langle E_{\gamma} \rangle = 3.4, 4.5$  and  $6.2$  MeV (panel (a), (b) and (c), respectively). The separation between the two most inner ridges, corresponding to the moment of inertia of the SD yrast band, is indicated by arrows.

the top and bottom panels of Fig. 2. Also in this case the intensity of the ridges (taken as the integral of the peak structure above a background extrapolated from the valley region) is higher when a high-energy  $\gamma$ -ray is detected in coincidence and the measured increase is of the same order as observed for the SD yrast line, as also discussed in connection with Fig. 4.

In a similar way as in normally deformed nuclei, most of the superdeformed rotational transitions emitted from highly excited states are expected to be damped, resulting in a strong fragmentation of the

$B(E2)$  strength out of each state [14,15]. These transitions form a continuous distribution of E2 character (E2 bump), which in the specific case of  $^{143}\text{Eu}$  is observed at  $1200 < E_{\gamma} < 1700$  keV. In  $^{143}\text{Eu}$  it is also found that the intensity of the superdeformed E2 bump is much stronger for transitions leading to the population of the low spin spherical (ND) structure as compared to that leading to the population of the low spin triaxial (TD) shape. In Fig. 3 we show 1D spectra obtained by projecting  $\gamma$ - $\gamma$  matrices, COR background subtracted and efficiency corrected, collecting the total population of  $^{143}\text{Eu}$  (label ND) and gated by TD low spin transitions. This has been done for average high-energy gating transitions of 3.4, 5.4 and 7.3 MeV (panel (a), (b) and (c), respectively), corresponding to the same intervals used for the SD yrast analysis. The TD spectra are obtained by gating on the 548, 853, 867, 884, 936 keV transitions, which are not populated by the decay-out of the SD states [14,17]. The ND and TD spectra are normalized to the intensity of the 553 keV low spinspherical transitions when a gating transition  $\langle E_{\gamma} \rangle = 7.3$  MeV is required. This normalization differs by 5% only from the 917 keV line previously used, and it was chosen because it is less contaminated in a spectrum compressed to 4 keV/ch. To evaluate the relative increase of the E2 bump we have used a procedure consistent with the one described in Ref. [14]. As shown in Fig. 3, we have evaluated the excess yield of the ND bump as compared to the TD bump, to isolate in the best possible way the expected contribution from the SD component only. In fact, as it was found in Ref. [14], the spectral shape of the TD contribution is very similar to that of the total spectrum measured at low  $\gamma$ -multiplicity, the latter (being at low spin) expected to contain a much reduced SD contribution. In addition, on the basis of the discrete line analysis one expects a sizable increase of the intensity of the SD component only. In the present work it is found that the total ND continuum spectrum shown in Fig. 3 increases by approximately 10% from panel (a) to panel (c), while the corresponding total TD spectrum decreases by approximately 20%. The excess yield between the ND and TD spectra (shown in the top panel of Fig. 3) is used to obtain the upper limit of the data points displayed in Fig. 4, which in the case of the highest energy gate corresponds to a value of  $\approx 1.6$ . Because of the difficulty in isolating the SD component from the total spectrum we have

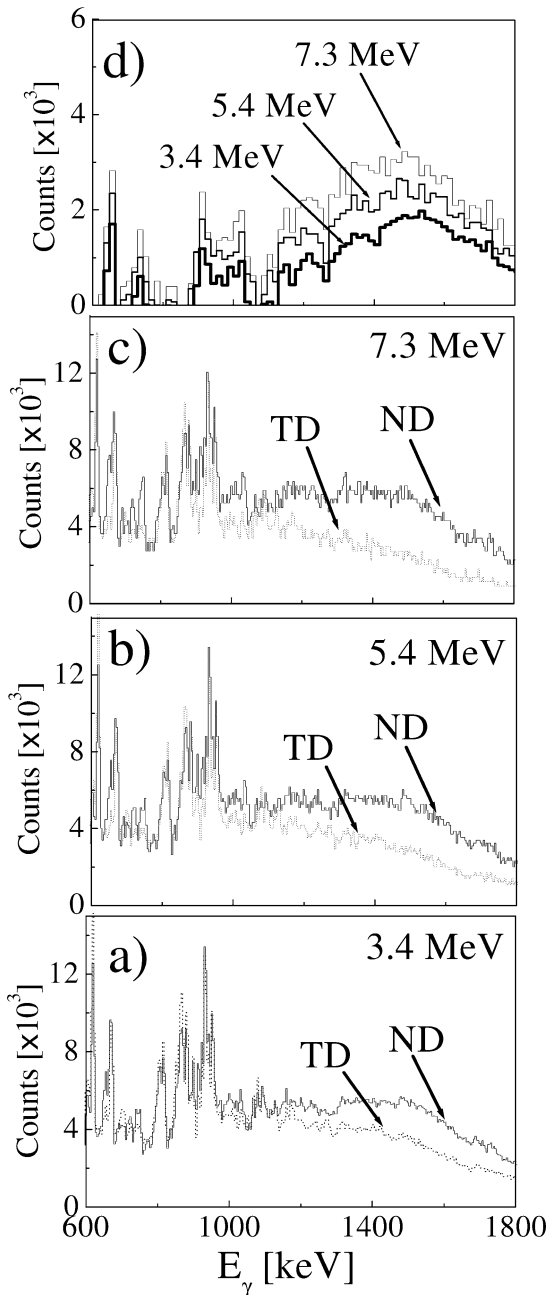


Fig. 3. Spectra of  $^{143}\text{Eu}$  collecting the entire decay flow (ND) and the triaxial contribution only (TD), gated by high-energy transition with  $\langle E_\gamma \rangle = 3.4, 4.5$  and  $7.3$  MeV (panel (a), (b) and (c), respectively). The intensity of the E2 bump observed in the ND spectra, obtained as a difference between the ND and TD spectra and normalized to the intensity of the 553 keV low spin spherical transition at the highest energy gating condition, is shown in the top part of the figure.

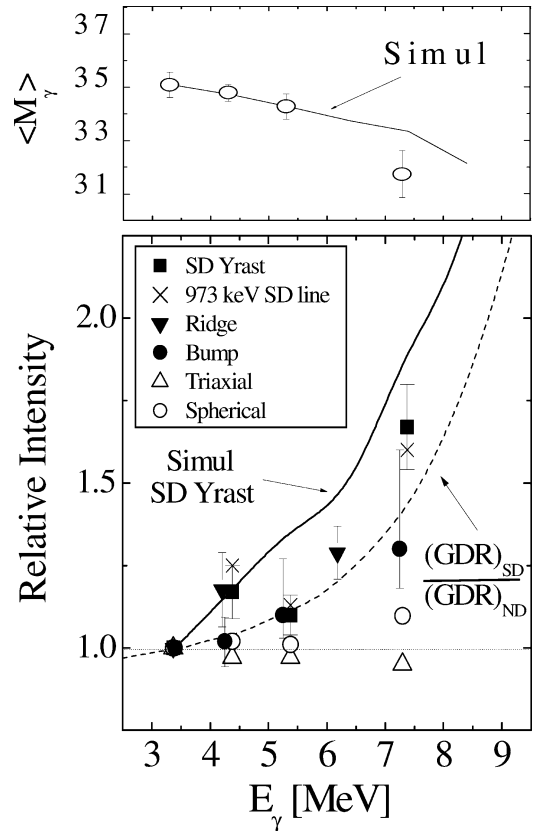


Fig. 4. The bottom part of the figure shows the intensity of the SD yrast (squares), of the SD ridge (filled triangles) and of the E2 bump (filled circles), as function of the energy of the gating transition, relative to the corresponding values measured at  $\langle E_\gamma \rangle = 3.4$  MeV. The cross symbols give the enhancement observed by using the well define 973 keV SD yrast line only. For comparison, the relative intensities of spherical (open squares) and triaxial (open triangles) low spin transitions are also given. The dashed line corresponds to the ratio of the strength functions of the GDR built on a SD and a ND nucleus, while the full line gives the predicted values of the relative intensity of the SD yrast, as obtained from the model of Refs. [10, 15]. In the top part of the figure the total average multiplicity of the  $\gamma$ -cascades leading to  $^{143}\text{Eu}$  is shown for both the experimental data (circles) and the model, as function of the energy of the gating transition.

evaluated the relative increase of the E2 bump using as a reference the same TD spectrum corresponding to the 3.4 MeV gate (shown in panel (a) of the figure). This gives an enhancement of the E2 continuum of  $\approx 1.3$  between the lowest and the highest gating conditions, as shown by full circles in Fig. 4. The lowest limit for the relative increase of the E2 bump has been

obtained by changing by 20% the COR background subtraction.

The intensity of the SD yrast, of the SD ridges and of the E2 bump, relatively to those measured at  $\langle E_\gamma \rangle = 3.4$  MeV, are shown in Fig. 4 with square, triangles and filled circles, respectively. Other experimental points corresponding to the average over the lower spin transitions of spherical shape (of energy 159, 176, 293, 728 and 955 keV, open circles) and triaxial shape (of energy 853, 867, 884 and 936 keV, open triangles), obtained with the same procedure used for the SD yrast lines, are shown in the figure for comparison. While in the case of transitions of the spherical and triaxially deformed configurations an approximately constant behaviour is found, with a value of  $\approx 1$ , an increase with  $\gamma$ -ray energy is instead measured in the case of the transitions of superdeformed nature. As shown in the top part of Fig. 4 by open circles, the total average multiplicity of the  $\gamma$ -cascades is found to decrease with increasing energy of the gating transitions, ruling out the possibility that the enhanced population of the SD structures could be due to a spin effect. On the other hand, if the increased population of the SD states is caused by the E1 feeding from excited states of the residual nucleus which has also an electric dipole vibration, one would expect a trend which follows the low energy tail of the GDR strength function. In Fig. 4 the ratio of the strength function of the superdeformed GDR ( $E_{1\text{GDR}} = 10.5$  MeV,  $\Gamma_{1\text{GDR}} = 3$  MeV with 33% of EWSR strength and  $E_{2\text{GDR}} = 17$  MeV,  $\Gamma_{2\text{GDR}} = 6.5$  MeV with 66% of EWSR) with the spherical GDR ( $E_{\text{GDR}} = 14.5$  MeV,  $\Gamma_{\text{GDR}} = 5$  MeV, 100% of EWSR), normalized to the data at 3.4 MeV, is shown by the dashed line. This represents the lowest limit expected for the situation in which the gating high-energy transition has a superdeformed nature and it is feeding directly the superdeformed structure. Indeed, it is found that the experimental data display the same trend as given by this simple estimate, although with slightly higher values. In order to understand such difference, which could be related to the complex  $\gamma$ -decay flow from the entry distribution of the residual nucleus down to the yrast line, we have performed schematic Monte Carlo simulation calculations. The adopted model, originally developed to study the feeding of the SD nucleus  $^{152}\text{Dy}$  [10], has earlier been used to describe the populations of the various spectral components of

the SD nucleus  $^{143}\text{Eu}$  [15], giving a good account for the experimental data. The model is based on the level densities of both ND and SD states, together with the E1 and E2 transition probabilities characteristic of the two deformed shapes. In the case of ND states the level density is described by the Fermi-gas expression of Ref. [23], with a level density parameter  $a_{\text{ND}} = A/10$ , while the level density of SD states is taken from the cranking + band mixing calculations of Ref. [24] (corresponding roughly to a level density parameter  $a_{\text{SD}} = A/18.6$ ). In the code, the two deformations are separated by a barrier, the tunneling through which allows the mixing between SD and ND states. In particular, the statistical E1 strength entering into the simulation is described as the tail of the giant dipole resonance of Lorentzian shape, with centroids and widths for the SD and ND configurations as given above. The parameters used in the calculations are the same as discussed in Ref. [15], with the only difference for the entry excitation energy, which has been increased by 5 MeV to match the new experimental condition. This gives a good reproduction of the population of the low spin ground state transition at 917 keV in  $^{143}\text{Eu}$ , for high-energy  $\gamma$ -rays ranging from 3 to 8 MeV.

As one can see in Fig. 4, the increase in the population of the SD yrast, as calculated by the simulation code (solid line), displays a trend similar to the simple estimate previously considered (dashed line) and in rather good agreement with the experimental data. In addition, as shown by the solid line in the top panel of Fig. 4, the total average multiplicity of the simulated cascades is also found to decrease with increasing energy of the gating transitions. Concerning spin effects, it has been found that an increase of the entry spin distribution produces a better population of the highest spin transitions of the SD yrast, ridge and E2 bump. Therefore, we can rule out spin effects as a possible explanation of our experimental observation, since our gating conditions correspond to a lowering of the spin distribution. On the other hand, since we have a sizable spin decrease ( $\approx 8$  units) at the highest-energy gating conditions, we have checked via simulation this effects on the population of SD yrast low spin transitions. It has been found that the total relative increase of the SD yrast population is of the order of 1–2% only.

The finding that the feeding intensity of the superdeformed yrast states is approximately 1.6 larger

when gating on high energy  $\gamma$ -rays (with  $E_\gamma > 6$  MeV), as compared to the ungated case, is the relevant result of this work. This is consistent with the fact that when an high-energy E1  $\gamma$ -ray is involved in the decay it is more likely connected with a SD rather than a ND nucleus. However, in order to obtain a full understanding of the feeding mechanism of the SD structures one needs a comparison with other mass regions and to investigate the competition with particle feeding.

### Acknowledgements

We wish to acknowledge the support from INFN, Italy, from the Danish Natural Science Research Council, from the Polish Scientific Committee (KBN Grant No. 2 P03B 118 22) and the EU Access to Large Scale Facilities-Training and Mobility of Research Program Contract No. ERBFMGECT980110, for INFN-Laboratori Nazionali di Legnaro.

### References

- [1] M. Carpenter, R.V.F. Janssens, Nucl. Phys. A 583 (1995) 183c.
- [2] P.J. Twin, Nucl. Phys. A 583 (1995) 199c.
- [3] B. Singh, R.B. Firestone, S.Y.F. Chu, Report No. LBL-38004, 1997.
- [4] G. Hackman et al., Phys. Rev. Lett. 79 (1997) 4100.
- [5] T.L. Khoo et al., Phys. Rev. Lett. 76 (1996) 1583.
- [6] A. Lopez-Martens et al., Phys. Lett. B 380 (1996) 18.
- [7] K. Schiffer, B. Herskind, J. Gascon, Z. Phys. A 332 (1989) 17.
- [8] J. Simpson et al., Phys. Rev. C 62 (2000) 024321.
- [9] M. Gallardo, M. Diebel, T. Døssing, R.A. Broglia, Nucl. Phys. A 443 (1985) 415.
- [10] B. Herskind et al., Phys. Rev. Lett. 59 (1987) 2416.
- [11] B. Hass et al., Phys. Lett. B 245 (1990) 13.
- [12] P. Taras et al., Phys. Rev. Lett. 61 (1988) 1348.
- [13] L.H. Zhu et al., Phys. Rev. C 55 (1997) 1169.
- [14] S. Leoni et al., Phys. Rev. Lett. 76 (1996) 3281.
- [15] S. Leoni et al., Phys. Lett. B 409 (1997) 71.
- [16] S. Leoni et al., Phys. Lett. B 498 (2001) 137.
- [17] A. Atac et al., Phys. Rev. Lett. 70 (1993) 1069.
- [18] A. Winther, Nucl. Phys. A 594 (1995) 203.
- [19] A. Maj et al., Nucl. Phys. A 571 (1994) 185.
- [20] D.C. Radford, Nucl. Instrum. Methods A 361 (1995) 297.
- [21] S.A. Forbes et al., Nucl. Phys. A 584 (1995) 149.
- [22] O. Andersen et al., Phys. Rev. Lett. 43 (1979) 687.
- [23] S. Aberg, Nucl. Phys. A 477 (1988) 18.
- [24] K. Yoshida, M. Matsuo, Nucl. Phys. A 612 (1997) 26.